Journal of the Korean Magnetic Resonance Society **2023**, *27*, 5-9
DOI 10.6564/JKMRS.2023.27.2.005

H-1, C-13, and N-15 resonance assignments of ENOD40B, a plant peptide hormone

Young Kee Chae*

Department of Chemistry, Sejong University, Seoul 05006, Republic of Korea

Received May 16, 2023; Revised Jun 10, 2023; Accepted Jun 10, 2023

Abstract ENOD40B, a plant peptide hormone, was doubly labeled with C-13 and N-15 by recombinant production in *Escherichia coli*. The peptide was prepared by affinity chromatography followed by protease cleavage and reverse-phase chromatography. To elucidate the mode of action against its receptor, sucrose synthase, we proceeded to assign the backbone and side-chain resonances using a set of double and triple resonance experiments. This result will be used to determine the three-dimensional structure of the peptide at its bound state as well as to observe the chemical shift changes upon binding.

Keywords plant peptide hormone, resonance assignment, sucrase synthase

Introduction

Legume plants have the ability to form symbiotic relationships with nitrogen-fixing bacteria such as *Rhizobium* species.[1] These bacteria have the ability to convert atmospheric nitrogen into a form usable by plants, and the symbiosis with legume was suggested for Mars soil stimultants.[2] Specialized structures called nodules found in the roots of legumes are where symbiosis between legumes and nitrogen-fixing bacteria occurs. Within these nodules, bacteria are surrounded by plant cells and receive nutrients and energy in exchange for fixed nitrogen.[3] ENOD40B is a 24-mer peptide hormone that comes into play in the formation of nodules.[4] Although the exact role of ENOD40B in the regulation of sucrose synthase activity during nodule formation in leguminous plants is still in question, it is evident that it binds to sucrose synthase in nodules to either enhance or inhibit the enzymatic activity.[5, 6]

In this study, we assigned H-1, C-13, and N-15 resonances of a free peptide to establish a basis for elucidation of the complex structure with its binding partner, sucrose synthase.

Experimental Methods

Sample preparation- The expression plasmid, pET28a/ubisac/ENOD40B, was constructed as reported previously.[7] The Rosetta(DE3)pLysS cells were used to produce the ubiquitin-ENOD40B fusion protein. Cells were let grown fully in a minimal medium supplemented with 1 g of $^{15}NH_4Cl$ and 1 g of $^{13}C_6$-glucose. Another 1 g of $^{13}C_6$-glucose was added to the culture with IPTG to the final concentration of 1 mM, and harvested by centrifugation 5 h later. The purification and cleavage of the fusion protein and the subsequent purification of the ENOD40B were performed as reported previously.[7] The lyophilized 3.4 mg of ENOD40B was dissolved in 0.5 mL of 10 mM sodium acetate pH 3.2 in 90% H_2O /10% D_2O to make a 2.5 mM

* Address correspondence to: **Young Kee Chae,** Department of Chemistry, Sejong University, Seoul 05006, Republic of Korea, Tel: 82-2-3408-3748; Fax: 82-2-3408-4317; E-mail: ykchae@sejong.ac.kr

peptide solution.

NMR experimentation - NMR spectra were collected at 298K on a Varian VNMRS 600MHz spectrometer equipped with a 5 mm triple resonance cryoprobe with z-axis gradient. Raw data were processed using the NMRPipe software.[8] The processed data were visualized and analyzed by POKY software.[9] Resonance assignments of [^{13}C, ^{15}N]-labeled ENOD40B was carried out by I-PINE through POKY.[10] The experiments performed included 2D ^{15}N-HSQC and ^{13}C-HSQC, and 3D triple resonance experiments such as HNCACB, CBCA(CO)NH, CCONH, HBHACONH, HCCONH, HCCH-TOCSY, and ^{15}N-NOESY experiments.[11-14] The experimental and processing parameters are listed in Table 1. Secondary or three-dimensional structure was predicted by TALOS-N or ESMFold (Evolutionary Scale Modeling) through POKY.[15, 16]

Results and Discussion

Sample preparation – The semi-stationary phase induction was employed in the production of doubly labeled ubiquitin-ENOD40B fusion protein. This was devised from the auto-induction medium where the included lactose acted as an inducer when the glucose was depleted.[17] However, the auto-induction medium is not economical when it comes to double labeling. In our previous publication, a stationary phase induction was employed where a fully grown culture was mixed with a fresh medium with the addition of IPTG.[18] In this project, we grew the culture with 1 g of ^{13}C-glucose, and added another 1 g with IPTG, and it worked fine. We could get 3.4 mg of doubly labeled peptide.

Resonance assignments - The resonances of [^{1}H-^{15}N] HSQC spectrum are labeled with residue types and numbers in Figure 1. We did not perform the HNCO experiment, which was unfortunate in terms of completeness, but it was not necessary in our sequential assignment process. The backbone assignments are summarized in Table 2. The side-chain assignments are provided in the supplementary materials. In summary, 23 of 24 HN or N, 23 of 24 CA, or 19 of 21 CB resonances were assigned. According to the I-PINE result, all assignments had 100 % probabilities except for the first residue, Met. As shown in Fig. 1, we could easily observe the indole Hε_1 at the bottom-left corner. Depending upon the pH and temperature, the side-chain NHs from Arg, His or Lys can be observed.[19] ENOD40B contains 3 Arg and 2 His. The 3 resonances at the upper right corner belong to these 3 Arg because they are often observed at pH values below 6 and the sample pH was 3.2. Although the histidine residues can be protonated below its pKa of 6, their Hδ_1/Hε_2 resonances are not observable due to the fast exchange with water. They can be observable if they are in the protein core or held tightly by the hydrogen bonds or salt bridges at the surface, which would not be the case of ENOD40B, so those resonances would not be observable. This would be the same for arginine Hη.

Secondary/tertiary structures – The secondary structure of ENOD40B predicted by TALOS-N implied a helix propensity at the N-terminus (Fig. 2a). This was also predicted by the ESMFold which also resulted in a helix at the N-terminus (Fig. 2b). The ESMFold predicted a helix from Val2 to Arg10 while the NMR predicted a helix from Glu5 to Arg10. The residues Val2, Leu3, and Glu4 showed mixed propensity according to the TALOS-N. This prediction was not expected because ENOD40B was a short 24-mer peptide without its binding receptor so that the overall structure would not be defined. However, the resonances in ^{15}N-HSQC spectrum were dispersed well, which might indicate at least a partial tertiary structure. The helical propensity was more visible when the secondary chemical shift analysis or PSIPRED prediction.[20, 21] On the other hand, the PACSY result showed only one residue (Val-12) in the hydrophobic core. All other residues were predicted to be solvent-exposed, which did not support the helical structure at the N-terminus. In summary, although it cannot be said definitively, ENOD40B is likely to have formed a helix structure

at the experimental condition. We included the sidechain assignments, sparky peak list files, results of PINE, PSIPRED, PECAN, and corresponding NMRSTAR files in the Supplementary materials. This work will be the basis for the structural and binding studies with the sucrose synthase, the receptor of ENOD40B. We will explore the structure of ENOD40B at its bound state.

Table 1. Experimental and processing parameters of employed double and triple resonance experiments. Asterisks (*) denote H-1 parameters.

Experiment	SW (Hz)			TD (acquisition, complex points)			TD (final, real points)		
	H	C	N	H	C	N	H	C	N
N-15 HSQC	12019		2000	1024		128	1024		256
C-13 HSQC	10000	6267		1024	64		2048	128	
HNCACB	12019	13000	2000	1024	96	48	614	256	128
CBCACONH	12019	13000	2000	512	60	56	307	256	128
HCCONH	12019	4500*	2000	512	64*	46	307	128*	128
CCONH	12019	12500	2000	512	64	48	307	128	48
HBHACONH	12019	5000*	2000	512	64*	48	307	128*	128
HCCH-TOCSY	12019	4500	12500*	512	56	56*	1024	128	128*

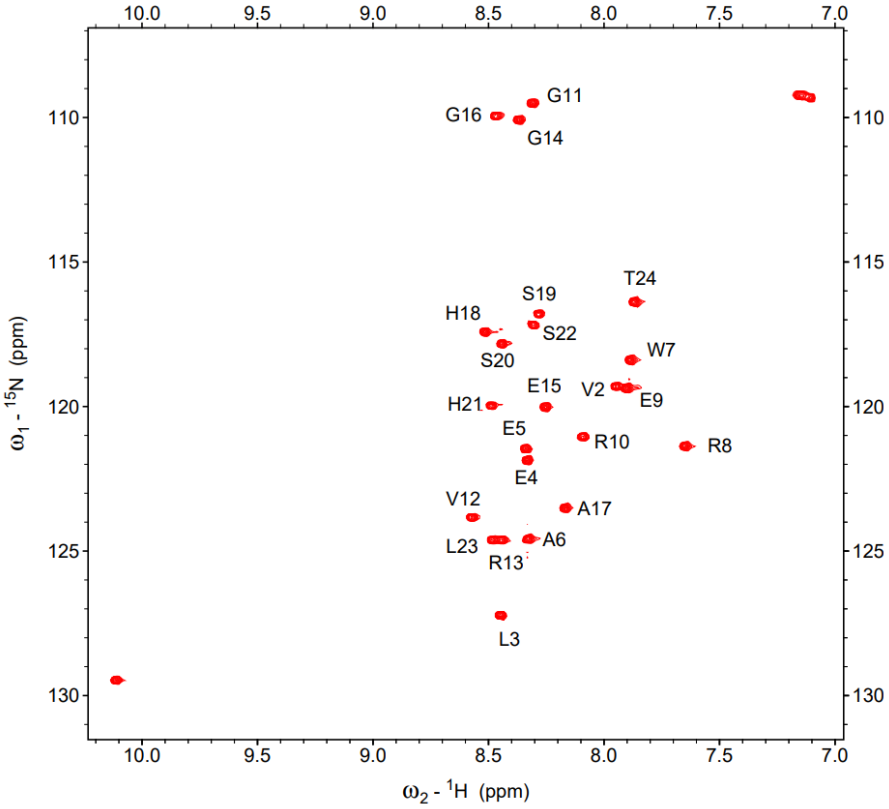

Figure 1. ^{1}H– ^{15}N HSQC spectra of $^{13}C/^{15}N$-ENOD40B in 10mM sodium acetate pH 3.2 at 298K. The backbone amide cross peaks are labeled with their corresponding residues. The resonances at lower left and upper right corners originated from the side-chains of W7 and R8/R10/R13, respectively.

Table 2. Backbone HN, N, C_α, C_β chemical shifts of ENOD40B (ppm)

Residue	HN	N	CA	CB	Residue	HN	N	CA	CB
1 Met			56.8		13 Arg	8.445	124.63	56.4	30.7
2 Val	7.949	119.31	62.3	32.7	14 Gly	8.37	110.09	45.2	
3 Leu	8.448	127.24	55	42.3	15 Glu	8.255	120.02	56	29.2
4 Glu	8.333	121.86	55.9	28.8	16 Gly	8.469	109.94	45.1	
5 Glu	8.34	121.47	56.1	28.7	17 Ala	8.17	123.51	52.5	19.1
6 Ala	8.329	124.57	53.5	18.6	18 His	8.517	117.42	55	28.8
7 Trp	7.89	118.39	57.8	28.8	19 Ser	8.284	116.79	58.1	64
8 Arg	7.652	121.37	56.8	30.5	20 Ser	8.444	117.82	58.4	63.7
9 Glu	7.906	119.36	56	28.7	21 His	8.49	119.95	55.1	28.9
10 Arg	8.093	121.06	56.5	30.7	22 Ser	8.307	117.16	58.3	63.8
11 Gly	8.309	109.51	44.5		23 Leu	8.485	124.64	55.5	42.3
12 Val	8.574	123.84	62.3	32.7	24 Thr	7.872	116.37		

(a)

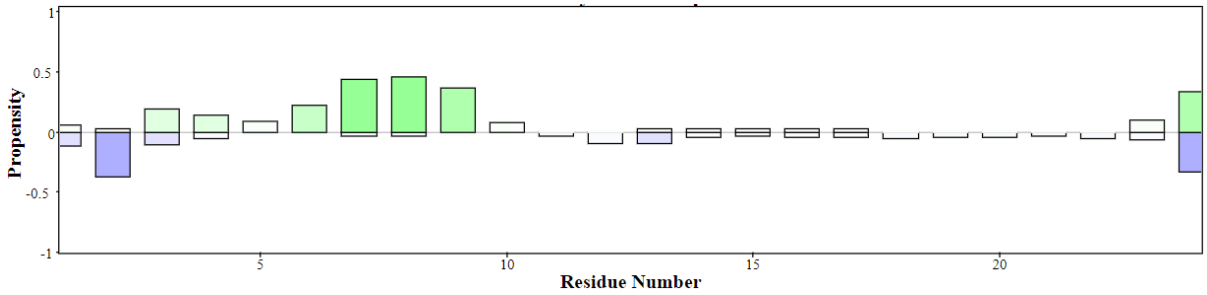

(b)

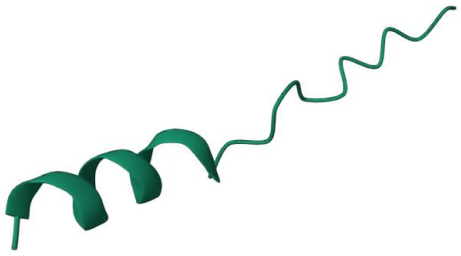

Figure 2. (a) Secondary structure prediction by TALOS-N. The positive values indicate the helix propensity. (b) Tertiary structure prediction by ESMFold (bottom). There is a helical structure at the N-terminus.

Supplementary Material

The Supplmentary Material is available free of charge at http://www.kmrs.or.kr/03_jkmrs/board01_list.html.

Acknowledgements

This work was supported by the National Research Foundation of Korea (NRF-2021R1F1A1046500), and the faculty research fund of Sejong University in 2023. The author thanks Dr. Marco Tonelli of the NMRFAM for his technical assistance.

References

1. Q. Wang, J. Liu, and H. Zhu, *Front. Plant Sci*. **9**, (2018)
2. R. Rainwater and A. Mukherjee, *PLoS One*. **16**, e0259957 (2021)
3. C. Masson-Boivin and J. L. Sachs, *Curr. Opin. Plant Biol.* **44**, 7 (2018)
4. Y. Matsubayashi and Y. Sakagami, *Annu. Rev. Plant Biol.* **57**, 649 (2006)
5. H. Rohrig, J. Schmidt, E. Miklashevichs, J. Schell, and M. John, *Proc. Natl. Acad. Sci. U.S.A.* **99**, 1915 (2002)
6. A. Kereszt, P. Mergaert, J. Montiel, G. Endre, and É. Kondorosi, *Front. Plant Sci.* **9**, 1026 (2018)
7. Y. K. Chae, M. Tonneli, and J. L. Markley, *Protein Pept. Lett.* **19**, 808 (2012)
8. F. Delaglio, S. Grzesiek, G. W. Vuister, G. Zhu, J. Pfeifer, and A. Bax, *J. Biomol. NMR.* **6**, 277 (1995)
9. W. Lee, M. Rahimi, Y. Lee, and A. Chiu, *Bioinformatics* (2021)
10. W. Lee, A. Bahrami, H. T. Dashti, H. R. Eghbalnia, M. Tonelli, W. M. Westler, and J. L. Markley, *J. Biomol. NMR.* **73**, 213 (2019)
11. M. Sattler, J. Schleucher, and C. Griesinger, *Prog. Nucl. Magn. Reson. Spectrosc.* **34**, 93 (1999)
12. S. Grzesiek and A. Bax, *J. Am. Chem. Soc.* **114**, 6291 (1992)
13. B. Kim and J. H. Kim, *J. Korean Magn. Reson. Soc.* **25**, 8 (2021)
14. J. E. Lee, G. H. Kim, and H. Won, *J. Korean Magn. Reson. Soc.* **25**, 58 (2021)
15. Y. Shen and A. Bax, *J. Biomol. NMR.* **56**, 227 (2013)
16. Z. Lin, H. Akin, R. Rao, B. Hie, Z. Zhu, W. Lu, N. Smetanin, R. Verkuil, O. Kabeli, Y. Shmueli; et al., *Science* **379**, 1123 (2023)
17. F. W. Studier, *Protein Expr. Purif.* **41**, 207 (2005)
18. Y. K. Chae, K. S. Cho, W. Chun, and K. Lee, *Protein Pept. Lett.* **10**, 369 (2003)
19. G. Platzer, M. Okon, and L. P. McIntosh, *J. Biomol. NMR.* **60**, 109 (2014)
20. L. J. McGuffin, K. Bryson, and D. T. Jones, *Bioinformatics*. **16**, 404 (2000)
21. D. S. Wishart, C. G. Bigam, A. Holm, R. S. Hodges, and B. D. Sykes, *J. Biomol. NMR.* **5**, 67 (1995)